Multiband Joint Detection with Correlated Spectral Occupancy in Wideband Cognitive Radios

Khalid Hossain, Ayman Assra, and Benoît Champagne, *Senior Member, IEEE*

Department of Electrical and Computer Engineering, McGill University, Montreal, PQ, Canada
E-mail: khalid.hossain@mail.mcgill.ca, ayman.assra@mail.mcgill.ca, benoit.champagne@mcgill.ca

***Abstract*— Recently, a wideband spectrum sensing scheme referred to as multiband joint detection has been proposed by Quan *et al.*, in which a set of frequency dependent detection thresholds are optimized to achieve the best trade-off between *aggregate* measures of opportunistic throughput and interference to primary users in cognitive radio (CR) networks. While this scheme shows significant performance gains over benchmark approaches, it employs a frequency-decoupled detector structure that is not optimal in the presence of correlation between subband occupancies, a common situation in CR applications. In this paper, we investigate how a frequency-coupled optimum linear energy combiner (OLEC) structure, recently proposed for single user scenarios, can be integrated into the above multiband joint detection framework to take further advantage of subband occupancy correlation in wideband spectrum sensing. We first analyze the performance of the single-user OLEC and derive expressions for its probabilities of false alarm and missed detection. Using these expressions, we then formulate joint optimization problems for the detection thresholds used by a bank of subband OLECs, with the aim to maximize the aggregate opportunistic throughput under interference constraints. Through numerical experiments with a Markov model of subband occupancy, we show that the use of the OLEC in wideband spectrum sensing can significantly enhance CR performance in terms of these global metrics, when compared to the decoupled multiband processing structure.**

I. Introduction

Cognitive radio (CR) is seen as a key enabling technology for the incorporation of dynamic spectrum access in future wireless networks [1], [2]. Indeed, by maintaining awareness of the radio environment through spectrum sensing and adjusting transmission parameters accordingly, CR can significantly improve communication efficiency and network throughput. In recent years, CR has gained further importance as it is an integral component of the IEEE 802.22 standard [3] and the focus of several other emerging applications [4].

By definition, CR terminals have built-in spectrum sensing capabilities that allow them to detect and opportunistically use *spectrum holes*, that is, momentarily silent portions of the licensed frequency spectrum. In this context, one refers to a user of the wireless system to which the frequency band has been licensed, such as a WLAN or broadcast television, as a *primary user* (PU), and to the CR of interest as a *secondary user* (SU). In order to maximize the opportunistic throughput without adding unacceptable level of interference to the PUs, spectrum sensing must be fast and accurate. In the literature, several approaches have been considered for this application, including matched filtering, feature extraction (e.g., cyclostationarity) and energy detection (ED) [5].

Because of its low implementation complexity and robustness to modeling assumption, ED has been favored in many recent studies, e.g. [6], [7], [8]. In this approach, the received signal energy in a given frequency band is used in a binary hypothesis test (i.e. compared to a threshold) to decide the occupancy state of that band. ED can be applied in both narrowband and wideband settings where in the latter case, it is typically performed by dividing the broad frequency band into smaller component subbands and performing narrowband detection in each subband independently [9].

Recently, *joint* multiband ED has shown great promises for spectrum sensing in CR networks [10], [11]. In particular, [10] introduces a scheme in which the information theoretic capacity and the cost of interfering with the PUs, for each subband, are applied to define global measures of *aggregate opportunistic throughput* and *aggregate interference*, respectively. This enables the design of an optimum set of detection thresholds that maximize the opportunistic throughput aggregated over all the subbands while keeping the aggregate interference under a prescribed level. The use of such jointly optimized thresholds leads to significant performance improvements over the use of fixed thresholds across all subbands.

ED approaches for wideband spectrum sensing currently employ a decoupled processing structure in which hypothesis-testing in any given subband is carried out based on the observed signal energy in that particular subband only, i.e., independently of the other available subband signals. This is so even for the above joint multiband schemes, where only the detection thresholds used in individual subbands are optimized from a wideband perspective. While the frequency-decoupled structure is optimal when the occupancies of the frequency subbands are independent of each other, this condition is rarely satisfied, especially in the presence of wideband PU signals, such as in broadcast television or WLAN [12].

To overcome this limitation in wideband spectrum sensing and improve detection performance, some authors have recently investigated new processing structure that can exploit correlation between the occupancies of frequency subbands [13]. For instance, [14] considers an autoregressive model to

Support for this work was provided by InterDigital Canada, the Natural Sciences and Engineering Research Council of Canada, and the Government of Québec under the PROMPT program.

978-1-4673-0762-8/12/$31.00 ©2012 IEEE

track the strengths of PU signals along frequencies and delimit their spectral support, which in turn facilitates ED over the identified bands. In [15], a novel detector structure is proposed in which multiband energy measurements from a CR terminal are linearly combined, using weights derived from a minimum mean-square error (MMSE) criterion, to form a summary statistic for binary detection in each subband. This frequency-coupled detector structure, referred to as the optimum linear energy combiner (OLEC), is shown to significantly outperform the traditional frequency-decoupled detector.

In this paper, we investigate how to integrate the OLEC detector [15] into the multiband joint detection framework of [10], in order to further exploit *a priori* knowledge of subband occupancy correlation in wideband spectrum sensing. We first analyze the performance of the OLEC detector [15] and derive closed-form expressions for its probabilities of false alarm and missed detection. Using these expressions, we then formulate joint optimization problems for the set of detection thresholds, with the aim to maximize the aggregate opportunistic throughput under interference constraints, or alternatively, minimize the aggregate interference under throughput constraints. Through numerical experiments, we demonstrate that the application of the OLEC in wideband spectrum sensing frameworks can significantly enhance the detection performance in terms of these global metrics, when compared to a decoupled multiband processing structure.

The rest of this paper is organized as follows. The system model is described in Section II. The single-user OLEC detector is discussed in Section III. In Section IV, the performance metrics of single-user OLEC detector are derived and subsequently applied in the formulation of the joint multiband optimization problem. The simulation results are presented in Section V. Finally, conclusions are drawn in Section VI.

II. Wideband System Model

We consider a scenario in which a CR unit detects the presence of a PU signal over a given wideband frequency range. Assuming a frame-based K-point discrete Fourier Transform (DFT) operation, the m-th sample of the signal observed by the SU in the k-th subband can be expressed as (see e.g. [16]):

$$R_k(m) = H_k S_k(m) + V_k(m), \tag{1}$$

where $k \in \{0, 1, \ldots, K-1\}$ is the frequency index, $m \in \{0, 1, \ldots, M-1\}$ is the frame index, and M is the total number of available frames for detection. In (1), $S_k(m)$, H_k and $V_k(m)$ respectively denote: the PU signal component in the k-th frequency subband at time m; the channel response between the PU and the SU; and the additive receiver noise. Following a common practice in the spectrum sensing literature (see, e.g., [6]), a probabilistic formulation is assumed for the signal and noise frequency samples. The signal samples of the PU, $\{S_k(m)\}$, and the background noise samples of the SU, $\{V_k(m)\}$, are modeled as independent random processes, whereby, for any given state of occupancy of the wideband channel, samples from each process are independent across frequency and frame indices, and obey a zero-mean complex circular Gaussian distribution. The noise variance, $\sigma_k^2 \triangleq E[|V_k(m)|^2]$, and the channel squared magnitude response, $G_k \triangleq |H_k|^2$, are assumed to be known from *a priori* estimation and to remain approximately constant during the processing interval. In the absence of a PU signal in subband k (hypothesis $\mathcal{H}_{0,k}$), we set $E[|S_k(m)|^2] = 0$, while in the presence of a PU signal in subband k (hypothesis $\mathcal{H}_{1,k}$), we set $E[|S_k(m)|^2] = 1$ without loss of generality. In the former case, (1) reduces in effect to $R_k(m) = V_k(m)$.

Here, we extend this formalism to take advantage of *a priori* knowledge about the state of occupancy of the multiple frequency subbands by the PU. Specifically, we model the occupancy of the k-th subband by means of a binary (indicator) random variable, B_k, with realization $b_k \in \{0, 1\}$, where 0 represents a spectrum hole, while 1 indicates the presence of the PU signal in the k-th subband. The multiband spectrum occupancy is represented by means of random vector:

$$\mathbf{B} = [B_0, B_1, \ldots, B_{K-1}]^T \tag{2}$$

with realizations $\mathbf{b} = [b_0, b_1, \ldots, b_{K-1}]^T \in \{0, 1\}^K$. We define the mean vector $\boldsymbol{\mu} = E[\mathbf{B}]$, with entries $\mu_i = E[B_i] = \Pr(B_i = 1)$, and the correlation matrix $\boldsymbol{\Lambda} = E[\mathbf{B}\mathbf{B}^T]$, with entries $\lambda_{i,j} = E[B_i B_j] = \Pr(B_i = B_j = 1)$. Note that the conditional signal power of the PU in the k-th subband, given the spectrum occupancy $\mathbf{B} = \mathbf{b}$, may be expressed compactly as $E[|S_k(m)|^2 | \mathbf{B} = \mathbf{b}] = b_k$. We assume that random vector $\mathbf{B}$ is independent of the noise processes, $\{V_k(m)\}$, and remains unchanged during the detection interval.

III. Single-User OLEC Dector

Within the above Bayesian framework, the maximum *a posteriori* (MAP) estimator of $\mathbf{B}$, given the observations $\{R_k(m)\}$ for $k \in \{0, \ldots, K-1\}$ and $m \in \{0, \ldots, M-1\}$, is developed in [15] and shown to be a function of the received signal energies in each subband over the M frames of interest, where the subband energies are given by:

$$Y_k = \sum_{m=0}^{M-1} |R_k(m)|^2. \tag{3}$$

In the special case where the subband occupancies are independent, i.e. $P_{\mathbf{B}}(\mathbf{b}) = \prod_{k=0}^{K-1} P_{B_k}(b_k)$, where $P_{B_k}(b_k) = \Pr(B_k = b_k)$, the multiband MAP estimator decouples into K parallel narrowband detectors, in which an independent scalar binary hypothesis test is performed on each subband energy Y_k. This assumption is commonly adopted in the context of wideband spectrum sensing. However, for the general case where the subband occupancies are correlated, the MAP detector leads to a non-linear integer optimization in K-dimensional space, with high computational complexity of order 2^K.

Alternatively, the frequency-coupled optimum linear energy combiner (OLEC) is proposed in [15] as a mean to exploit the correlation between subband occupancies in the single-user detection process, without the computational cost of the MAP estimator. In this approach, B_k is estimated as

an affine transformation of the random energy vector $\mathbf{Y} = [Y_0, Y_1, \ldots, Y_{K-1}]^T$:

$$\hat{B}_k = \boldsymbol{\xi}_k^T \mathbf{Y} + \epsilon_k, \tag{4}$$

where the weight vector $\boldsymbol{\xi}_k$ and affine coefficient ϵ_k are optimized for best performance. The optimum weight vector in the minimum mean-square error (MMSE) sense, i.e. minimizing the objective $J(\boldsymbol{\xi}_k, \epsilon_k) = E[(\hat{B}_k - B_k)^2]$, is obtained as:

$$\boldsymbol{\xi}_k^o = E[\bar{\mathbf{Y}}\bar{\mathbf{Y}}^T]^{-1} E[\bar{\mathbf{Y}}\bar{B}_k] \tag{5}$$

where we define the centered quantities $\bar{\mathbf{Y}} = \mathbf{Y} - E[\mathbf{Y}]$ and $\bar{B}_k = B_k - \mu_k$, while the optimum value of ϵ_k is given by $\epsilon_k^o = \mu_k - \boldsymbol{\xi}_k^{oT} E[\mathbf{Y}]$.

Convenient expressions for the various moments needed in (5) are derived as follows. We first note that under the signal model assumptions in Section II, we have $E[|S_i(m)|^2] = E[E[|S_i(m)|^2 | B_i]] = E[B_i] = \mu_i$, $i \in \{0 \ldots, K-1\}$. Then, using (1) and (3), we obtain:

$$E[Y_i] = E\big[\sum_{m=0}^{M-1} |R_i(m)|^2\big] = M\big(\mu_i G_i + \sigma_i^2\big). \tag{6}$$

To evaluate $E[B_k Y_i]$, we observe that $E[B_k |S_i(m)|^2] = E[E[B_k |S_i(m)|^2 | \mathbf{B}]] = E[B_k B_i] = \lambda_{i,k}$. Again, using (1) and (3), we can write:

$$E[B_k Y_i] = E\big[B_k \sum_{m=0}^{M-1} |R_i(m)|^2\big] = M\big(\lambda_{i,k} G_i + \mu_k \sigma_i^2\big). \tag{7}$$

Then, using (6) and (7), we obtain

$$\begin{aligned} E[\bar{B}_k \bar{Y}_i] &= E[B_k Y_i] - E[B_k] E[Y_i] \\ &= M\big(\lambda_{i,k} - \mu_i \mu_k\big) G_i. \end{aligned} \tag{8}$$

Next, we consider the moment $E[Y_i Y_j]$. As before, using (1) and (3), we have

$$\begin{aligned} E[Y_i Y_j] &= \sum_{m=0}^{M-1} \sum_{m'=0}^{M-1} E\big[|R_i(m)|^2 |R_j(m')|^2\big] \\ &= M^2 G_i G_j E[B_i B_j] + M G_i G_i E[B_i] \delta_{i,j} \\ &\quad + M^2 G_i \sigma_j^2 E[B_i] + 2M G_i \sigma_i^2 E[B_i] \delta_{i,j} \\ &\quad + M^2 G_j \sigma_i^2 E[B_j] + M(M + \delta_{i,j}) \sigma_i^2 \sigma_j^2 \end{aligned} \tag{9}$$

where $\delta_{i,j} = 1$ if $i = j$ and 0 otherwise. The above derivation makes use of a standard formula for the 4th moment of jointly Gaussian complex circular random variables [17], [18]. Using (9), we finally obtain

$$\begin{aligned} E[\bar{Y}_i \bar{Y}_j] &= E[Y_i Y_j] - E[Y_i] E[Y_j] \\ &= M^2 \big(\lambda_{i,j} - \mu_i \mu_j\big) G_i G_j \\ &\quad + M(G_i^2 \mu_i + 2 G_i \sigma_i^2 \mu_i + \sigma_i^4) \delta_{i,j}. \end{aligned} \tag{10}$$

Using (4) and (5), the resulting OLEC detector for the K subbands can be represented by the following hypothesis tests:

$$Z_k = \boldsymbol{\xi}_k^{oT} \mathbf{Y} \underset{\mathcal{H}_{0,k}}{\overset{\mathcal{H}_{1,k}}{\gtrless}} \gamma_k, \quad k = 0, 1, ..., K-1 \tag{11}$$

where, for convenience, the bias term ϵ_k^o is absorbed in the detection threshold γ_k. The OLEC detector is computationally much simpler than joint MAP detection, yet its use of the MMSE linear combiner weight vector $\boldsymbol{\xi}_k^o$ from (5) ensures that available *a priori* knowledge – about the state of occupancy of the multiple subbands comprising the frequency band of interest – is exploited optimally.

IV. Single-User Multiband joint detection

Our objective is to develop an efficient detector that will enable the SU to determine the wideband PU's spectrum occupancy, which is tantamount to estimating the unknown value of binary vector $\mathbf{B}$. This problem has been considered in [10], where the aim is to jointly design a set of detection thresholds that maximize the opportunistic throughput aggregated over all the subbands, while keeping the aggregate interference under a critical value. However, the resulting scheme employs a decoupled processing structure, which neglects the correlation between subband occupancies. In [15], it is demonstrated that the use of the frequency-coupled OLEC detector can lead to substantial improvement in detection performance over the traditional decoupled structure used in the existing literature.

Here, we consider the use of the OLEC detector (11) in a multiband joint detection framework. We proceed in two steps: (1) We derive the probabilities of false alarm and missed detection in each subband of the single-user OLEC detector; (2) We optimize the detection thresholds used in the different subbands via the joint multi-band approach in [10].

A. Performance Metrics

In the present context, a false alarm in the kth subband refers to a situation where a decision is made in favor of $\mathcal{H}_{1,k}$ (occupied band) when $\mathcal{H}_{0,k}$ is actually true (spectrum hole); while a missed detection refers to the opposite situation, i.e. deciding in favor of $\mathcal{H}_{0,k}$ when $\mathcal{H}_{1,k}$ is true. For M large, the central limit theorem dictates that Y_k in (3), and hence, Z_k (11), are approximately normally distributed under each hypothesis. Therefore, the probabilities of false alarm and missed detection associated with (11) can be expressed as:

$$P_f^{(k)}(\gamma_k) = Q\bigg(\frac{\gamma_k - E[Z_k | B_k = 0]}{\sqrt{Var[Z_k | B_k = 0]}}\bigg), \tag{12}$$

$$P_m^{(k)}(\gamma_k) = 1 - Q\bigg(\frac{\gamma_k - E[Z_k | B_k = 1]}{\sqrt{Var[Z_k | B_k = 1]}}\bigg), \tag{13}$$

where $Q(x) \triangleq (1/\sqrt{2\pi}) \int_x^\infty e^{-t^2/2} dt$ and

$$E[Z_k | B_k = b_k] = \boldsymbol{\xi}_k^{oT} E[\mathbf{Y} | B_k = b_k], \tag{14}$$

$$Var[Z_k | B_k = b_k] = \boldsymbol{\xi}_k^{oT} E[\bar{\mathbf{Y}}\bar{\mathbf{Y}}^T | B_k = b_k] \boldsymbol{\xi}_k^o. \tag{15}$$

Similar to (6)-(10), it can be shown that:

$$E[Y_i | B_k = b_k] = M(\mu_{i|k} G_i + \sigma_i^2), \tag{16}$$

$$\begin{aligned} E[\bar{Y}_i \bar{Y}_j | B_k = b_k] &= M^2 G_i G_j (\lambda_{i,j|k} - \mu_{i|k} \mu_{j|k}) \\ &\quad + M(\mu_{i|k} G_i^2 + 2\mu_{i|k} G_i \sigma_i^2 + \sigma_i^4) \delta_{i,j}, \end{aligned} \tag{17}$$

where $\mu_{i|k} \equiv E[B_i|B_k = b_k]$, and $\lambda_{i,j|k} \equiv E[B_iB_j|B_k = b_k]$. These conditional moments may be empirically measured in a live network or computed using a suitable occupancy model.

B. OLEC-Based Multiband Joint Detection

Here, we consider a multiband joint detection framework where we seek the optimum use of the unoccupied spectrum without introducing undesirable interference to the PU systems. In order to achieve this, we quantify the net spectrum use and the net interference addition using two global (i.e., wideband) metrics, as originally proposed in [10]. Using (11)-(13), we begin by defining the following vectors:

$$\boldsymbol{\gamma} = [\gamma_0, \gamma_1, \ldots, \gamma_{K-1}]^T, \tag{18}$$

$$\mathbf{P}_f(\boldsymbol{\gamma}) = [P_f^{(0)}(\gamma_0), \ldots, P_f^{(K-1)}(\gamma_{K-1})]^T, \tag{19}$$

$$\mathbf{P}_m(\boldsymbol{\gamma}) = [P_m^{(0)}(\gamma_0), \ldots, P_m^{(K-1)}(\gamma_{K-1})]^T. \tag{20}$$

Using these notations, the *aggregate opportunistic throughput* available to the SU and the *aggregate interference* to the PU can be defined as follows, respectively:

$$R(\boldsymbol{\gamma}) \triangleq \mathbf{r}^T[\mathbf{1} - \mathbf{P}_f(\boldsymbol{\gamma})], \tag{21}$$

$$C(\boldsymbol{\gamma}) \triangleq \mathbf{c}^T\mathbf{P}_m(\boldsymbol{\gamma}). \tag{22}$$

In (21), vector $\boldsymbol{r} = [r_0, r_1, \ldots, r_{K-1}]^T$, where $r_k \geq 0$ represents the throughput achievable over the k-th subband by the SU. The value of r_k can be determined from experimental measurements (channel sounding) in a given radio environment or, otherwise, estimated using Shannon theoretic capacity formula [19]. In (22), vector $\boldsymbol{c} = [c_0, c_1, \ldots, c_{K-1}]^T$, where $c_k \geq 0$ represents the cost associated with interfering with the PU in the k-th subband. Given these global metrics, we seek a jointly optimum set of detection thresholds, $\boldsymbol{\gamma}$, that achieves one of the following:

- Maximize the aggregate opportunistic throughput given an upper bound, $\epsilon > 0$, on the aggregate interference;
- Minimize the aggregate interference given a lower bound, $\delta > 0$, on the aggregate opportunistic throughput.

Furthermore, in order to limit the interference and achieve a minimum opportunistic utilization in each subband, we impose the constraints:

$$P_m^{(k)}(\gamma_k) \leq \alpha_k, \quad P_f^{(k)}(\gamma_k) \leq \beta_k \tag{23}$$

for $k = 0, 1, \ldots, K-1$, where it is realistic to assume $0 \leq \alpha_k \leq 1/2$ and $0 \leq \beta_k \leq 1/2$. Using (12)-(13) and the fact that the function $Q(x)$ is monotonically decreasing, the above constraints on $P_m^{(k)}(\gamma_k)$ and $P_f^{(k)}(\gamma_k)$ can be transformed into the following linear constraints on the feasible set of the threshold vector $\boldsymbol{\gamma}$:

$$\gamma_{min,k} \leq \gamma_k \leq \gamma_{max,k} \tag{24}$$

$$\gamma_{min,k} \triangleq E[Z_k|B_k = 0] + Q^{-1}(\beta_k)\sqrt{Var[Z_k|B_k = 0]},$$

$$\gamma_{max,k} \triangleq E[Z_k|B_k = 1] + Q^{-1}(1 - \alpha_k)\sqrt{Var[Z_k|B_k = 1]},$$

where the expressions for the conditional mean and variance of Z_k are available from Section IV-A. Therefore, the multiband joint optimization problems can be formulated as follows:

TABLE I

POWER DELAY PROFILE OF 4-PATH FREQUENCY-SELECTIVE FADING CHANNEL IN A SINGLE-USER CR NETWORK

Delays (ns)	0	20	50	120
Av. Power Gain (dB)	-2	-8	-19	-21

- Maximization of aggregate opportunistic throughput with constraint on aggregate interference:

$$\max_{\boldsymbol{\gamma}} R(\boldsymbol{\gamma}) \text{ s.t. } C(\boldsymbol{\gamma}) \leq \epsilon,\ \gamma_{min,k} \leq \gamma_k \leq \gamma_{max,k} \tag{25}$$

- Minimization of aggregate interference with constraint on aggregate opportunistic throughput:

$$\min_{\boldsymbol{\gamma}} C(\boldsymbol{\gamma}) \text{ s.t. } R(\boldsymbol{\gamma}) \geq \delta,\ \gamma_{min,k} \leq \gamma_k \leq \gamma_{max,k} \tag{26}$$

V. NUMERICAL RESULTS

In this section, numerical results are presented to evaluate the comparative performance of the frequency-coupled OLEC-based detector and the traditional frequency-decoupled detector within the multiband joint optimization framework of [10].

We consider a wideband frequency spectrum of 48 MHz bandwidth, which is equally divided into $K = 8$ subbands. For each subband, the maximum probabilities of missed detection and false alarm are set to $\alpha_k = 0.2$ and $\beta_k = 0.5$, respectively. We model the correlation between subband occupancies using a homogeneous Markov chain defined over the discrete frequency index k. The initial occupancy state of the chain, B_0, is set to 1 with probability $P_{B_0}(1) = 0.5$, while the occupancy states at frequencies $k = 1, \ldots, K-1$ are generated by means of a binary symmetric transition model with parameter p denoting the probability of a change in occupancy, that is: $P_{B_{k+1}|B_k}(1|0) = P_{B_{k+1}|B_k}(0|1) = p$. Given this model, the moments μ_i, $\mu_{i|k}$, $\lambda_{i,j}$ and $\lambda_{i,j|k}$ introduced in Section II and Section IV can be derived analytically, and subsequently $P_f^{(k)}(\gamma_k)$ and $P_m^{(k)}(\gamma_k)$ can be computed exactly from (12) and (13) respectively.

The correlation coefficient between neighboring subband occupancies, B_k and B_{k+1}, is set to $\rho = 1 - 2p = 0.7$. The channel between the PU and CR experiences frequency-selective fading with $L = 4$ resolvable paths, where the delay and average power gain for each path are given in Table I. The additive noise power σ_k^2 is normalized to 1. The design parameters for the multiband joint detection, i.e. the channel squared magnitude, the opportunistic rate (in kbps) and the interference penalty for each subband, are given in Table II. Finally, $M = 100$ frames are used to compute the subband energies. The numerical results presented in this section are produced by solving the above inequality-constrained convex optimization problems (25) and (26). Efficient numerical search algorithms such as the interior-point method can be used to find the optimum solution. In our work, we use the MATLAB routine `fmincon`, which provides implementations of several constrained minimization algorithms [20].

Fig. 1 plots the maximum aggregate opportunistic throughput achievable by the SU against the constraint ϵ on the aggregate interference to the PU. By exploiting *a priori*

TABLE II

PARAMETERS USED IN THE SINGLE-USER MULTIBAND JOINT DETECTION EXPERIMENT

k	0	1	2	3	4	5	6	7
G_k	0.61	0.49	0.35	0.25	0.23	0.35	0.52	0.59
r_k	612	524	623	139	451	409	909	401
c_k	1.91	8.17	4.23	3.86	7.16	6.05	0.82	1.30

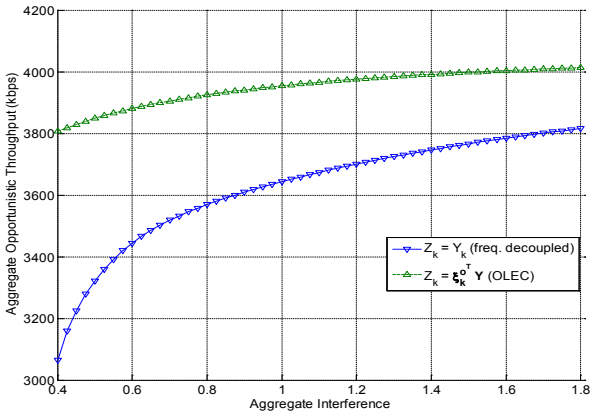

Fig. 1. Maximum aggregate opportunistic throughput of SU against the constraint on aggregate interference to PU.

knowledge of the correlation between subband occupancies, the frequency-coupled OLEC detector ($Z_k = \boldsymbol{\xi}_k^{oT}\mathbf{Y}$) results in significant throughput enhancement over the traditional frequency-decoupled scheme in [10] ($Z_k = Y_k$), and this over a wide range of interference constraints. The same argument is extended to a scenario where the SU targets a specific aggregate opportunistic throughput with minimal attainable aggregate interference, as shown in Fig. 2. That is, the use of the OLEC in multiband joint ED reduces the interference level imposed on the PU, especially at higher data rates.

VI. CONCLUSION

In this paper, we have presented a multiband joint detection scheme based on the OLEC detector for wideband CRs. The proposed scheme, which employs a frequency-coupled processing structure, has the advantage of exploiting *a priori* knowledge of subband occupancy correlation in making its sensing decisions across a wide frequency band. Through numerical experiments, we showed that OLEC-based multiband joint detector can significantly enhance the performance of high data-rate CR networks. The extension of the proposed OLEC-based multiband joint ED approach to multiple cooperating CR terminals is currently under investigation as a means to overcome the deleterious effects of multipath fading and shadowing in wideband spectrum sensing.

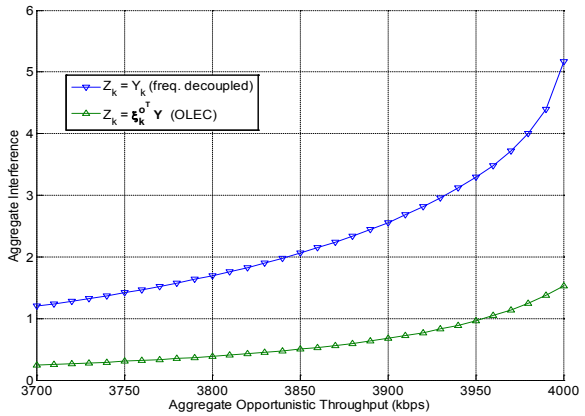

Fig. 2. Minimum aggregate interference to PU against the constraint on aggregate opportunistic throughput of SU.

REFERENCES

[1] S. Haykin, "Cognitive radio: brain-empowered wireless communications", *IEEE J. Sel. Areas in Communication*, vol. 23, no. 2, pp. 201–220, Feb. 2005.

[2] T. Yücek and H. Arslan, "A survey of spectrum sensing algorithms for cognitive radio applications", *IEEE Communications Surveys & Tutorials*, vol. 11, no. 1, pp. 116–130, Mar. 2009.

[3] C. Cordeiro, K. Challapali, D. Birru, and S. Shankar, "IEEE 802.22: An introduction to the first wireless standard based on cognitive radios", in *J. of Communications*, Apr. 2006, vol. 25, pp. 38–47.

[4] J. Wang, M. Ghosh, and K. Challapali, "Emerging cognitive radio applications: A survey", *IEEE Communications Magazine*, vol. 49, no. 3, pp. 74–81, 2011.

[5] Z. Quan, S. Cui, H. V. Poor, and A. H. Sayed, "Collaborative wideband sensing for cognitive radios", *IEEE Signal Processing Magazine*, vol. 25, no. 6, pp. 60–73, Nov. 2008.

[6] A. Ghasemi and E.S. Sousa, "Collaborative spectrum sensing for opportunistic access in fading environments", in *Proc. IEEE Int. Symp. New Frontiers in Dynamic Spectrum Access Networks*, Nov. 2005, pp. 131–136.

[7] R. Chen, J.-M. Park, and K. Bian, "Robust distributed spectrum sensing in cognitive radio networks", in *Proc. 27th Conf. Computer Communications (INFOCOM)*, Apr. 2008, pp. 1876–1884.

[8] S. Atapattu, C. Tellambura, and H. Jiang, "Energy detection based cooperative spectrum sensing in cognitive radio networks", *IEEE Trans. Wireless Communications*, vol. 10, no. 4, pp. 1232–1241, Apr. 2011.

[9] A. Taherpour, S. Gazor, and M. Nasiri-Kenari, "Invariant wideband spectrum sensing under unknown variances", *IEEE Trans. Wireless Communications*, vol. 8, no. 5, pp. 2182–2186, May 2009.

[10] Z. Quan, S. Cui, A. H. Sayed, and H. V. Poor, "Optimal multiband joint detection for spectrum sensing in cognitive radio networks", *IEEE Trans. Signal Processing*, vol. 57, no. 3, pp. 1128–1140, Mar. 2009.

[11] P. P.-Hoseini and N. C. Beaulieu, "Optimal wideband spectrum sensing framework for cognitive radio systems", *IEEE Trans. Signal Processing*, vol. 59, no. 3, pp. 1170–1182, Mar. 2011.

[12] B.-J. Kang, "Spectrum sensing issues in cognitive radio networks", in *Int. Symp. Communications and Information Technology*, Jan. 2009, pp. 824–828.

[13] H. Li and R. C. Qiu, "A graphical framework for spectrum modeling and decision making in cognitive radio networks", in *Proc. of IEEE GLOBECOM Conf.*, Dec. 2010, pp. 1–6.

[14] C.-H. Hwang, G.-L. Lai, and S.-C. Chen, "Spectrum sensing in wideband OFDM cognitive radios", *IEEE Trans. Signal Processing*, vol. 58, no. 2, pp. 709–719, Feb. 2010.

[15] K. Hossain and B. Champagne, "Wideband spectrum sensing for cognitive radios with correlated subband occupancy", *IEEE Signal Processing Letters*, vol. 18, no. 1, pp. 35–38, Jan. 2011.

[16] J. C. Park, J. S. Wang, H. G. Kang, S. Yoon, I. Song, and Y. H. Kim, "Detection of variable subband nulling mode for OFDM-based cognitive radio in narrowband interference channels", *IEEE Trans. Wireless Communications*, vol. 10, no. 3, pp. 782–791, Mar. 2011.

[17] R. A. Monzingo and T. Miller, *Introduction to Adaptive Arrays*, SciTech Publishing, 2004.

[18] I. S. Reed, "On a moment theorem for complex gaussian processes", *IRE Trans. Information Theory*, vol. 8, no. 3, pp. 194 – 195, May 1962.

[19] A. Goldsmith, *Wireless Communications*, Cambridge University Press, 2006.

[20] MathWorks, "Matlab User's Guide, available online: http://www.mathworks.com/help/toolbox/optim/ug/fmincon.html".